THE JOURNAL OF BIOLOGICAL CHEMISTRY VOL. 283, NO. 20, pp. 14153–14164, May 16, 2008

Effector Proteins Exert an Important Influence on the Signaling-active State of the Small GTPase Cdc42*

Received for publication, July 30, 2007, and in revised form, February 25, 2008 Published, JBC Papers in Press, March 18, 2008, DOI 10.1074/jbc.M706271200

Matthew J. Phillips[‡], **Guillermo Calero**[§], **Britton Chan**[‡], **Sekar Ramachandran**[‡], **and Richard A. Cerione**[‡¶1]

From the [‡]*Department of Chemistry and Chemical Biology, Baker Laboratory,* [¶]*Department of Molecular Medicine, College of Veterinary Medicine, Cornell University, Ithaca, New York 14853 and the* [§]*Department of Structural Biology, Stanford University School of Medicine, Stanford, California 94305*

GTP-binding (G) proteins regulate the flow of information in cellular signaling pathways by alternating between a GTP-bound "active" state and a GDP-bound "inactive" state. Cdc42, a member of the Rho family of Ras-related small G-proteins, plays key roles in the regulation of cell shape, motility, and growth. Here we describe the high resolution x-ray crystal structure for Cdc42 bound to the GTP analog guanylyl β,γ-methylene-diphosphonate (GMP-PCP) (*i.e.* the presumed signaling-active state) and show that it is virtually identical to the structures for the signaling-inactive, GDP-bound form of the protein, contrary to what has been reported for Ras and other G-proteins. Especially surprising was that the GMP-PCP- and GDP-bound forms of Cdc42 did not show detectable differences in their Switch I and Switch II loops. Fluorescence studies using a Cdc42 mutant in which a tryptophan residue was introduced at position 32 of Switch I also showed that there was little difference in the Switch I conformation between the GDP- and GMP-PCP-bound states (*i.e.* <10%), which again differed from Ras where much larger changes in Trp-32 fluorescence were observed when comparing these two nucleotide-bound states (>30%). However, the binding of an effector protein induced significant changes in the Trp-32 emission specifically from GMP-PCP-bound Cdc42, as well as in the phosphate resonances for GTP bound to this G-protein as indicated in NMR studies. An examination of the available structures for Cdc42 complexed to different effector proteins, *versus* the x-ray crystal structure for GMP-PCP-bound Cdc42, provides a possible explanation for how effectors can distinguish between the GTP- and GDP-bound forms of this G-protein and ensure that the necessary conformational changes for signal propagation occur.

Cdc42 is a member of the Rho family of Ras-related small G-proteins and is an essential protein found in all eukaryotic organisms, including yeast, flies, and mammals (1–3). Like Ras, the founding member of the small G-protein family (4), Cdc42 undergoes a GTP-binding/GTP-hydrolytic cycle that enables it to act as a molecular switch in cells. It is activated to undergo GDP-GTP exchange by members of the Dbl family of guanine nucleotide exchange factors (5–7). GTP-bound Cdc42 can bind and/or activate over 20 downstream effector proteins that are responsible for mediating a diversity of cellular functions, including actin cytoskeletal remodeling, cell polarity, intracellular trafficking, epidermal growth factor receptor degradation, and cell cycle progression (1–3, 8). These different signals are terminated when Cdc42 is deactivated through its ability to hydrolyze GTP, a reaction that is catalyzed by GTPase-activating proteins (GAPs)[2] (9).

Structural studies of a number of GTP-binding proteins, beginning with the bacterial elongation factor Ef-Tu, and including H-Ras and the α subunits of various members of the family of large G-proteins, have shown that a conserved architecture exists for GTP binding and hydrolytic activity, comprising five α-helices and six β-strands (10–14). Moreover, comparisons of the x-ray crystal structures for many of these proteins bound to GDP and GTP analogs highlighted two regions called Switch I and Switch II that change their conformation upon GDP-GTP exchange. In the case of H-Ras and related small G-proteins, Switch I encompasses residues 30–38 within the α1-β2 loop, whereas Switch II is made up of residues 60–76 within β3-α2 (12, 15). It has been commonly assumed that changes in these Switch regions represent the underlying basis for GTP-dependent signal propagation, and indeed Switch I has been shown to be a principal site used by Ras and related small G-proteins, including Cdc42, to engage their downstream effectors.

Given the shared architecture between Ras, Cdc42, and other Rho family small G-proteins, there was every reason to expect that Cdc42 would exhibit the same types of GTP-dependent changes in Switch I and II, as originally described for H-Ras. However, surprisingly, we found that this was not the case. The high resolution x-ray crystal structure for Cdc42 complexed to the nonhydrolyzable GTP analog GMP-PCP was virtually identical to that for Cdc42 bound to GDP, despite the fact that only GMP-PCP-bound Cdc42 and not its GDP-bound counterpart was able to productively engage effector proteins. Likewise, we found that Cdc42 molecules containing a tryptophan residue

* This work was supported, in whole or in part, by National Institutes of Health Grants GM40654 and GM47458 (to R. A. C.). The costs of publication of this article were defrayed in part by the payment of page charges. This article must therefore be hereby marked "*advertisement*" in accordance with 18 U.S.C. Section 1734 solely to indicate this fact.

The atomic coordinates and structure factors (code 2QRZ) have been deposited in the Protein Data Bank, Research Collaboratory for Structural Bioinformatics, Rutgers University, New Brunswick, NJ (http://www.rcsb.org/).

[1] To whom correspondence should be addressed. Tel.: 607-253-3888; Fax: 607-253-3659; E-mail: rac1@cornell.edu.

[2] The abbreviations used are: GAP, GTPase-activating protein; GTPγS, guanosine 5′-3-*O*-(thio)triphosphate; GMP-PCP, guanylyl β,γ-methylene-diphosphonate; GMP-PNP, guanosine-5′-[(β,γ)-imido]triphosphate; MES, 4-morpholineethanesulfonic acid; PDB, Protein Data Bank; PBD, p21-binding domain; GST, glutathione *S*-transferase; r.m.s.d., root mean square deviation; CRIB, Cdc42/Rac-interactive binding; Pak, p21-activated kinase.

inserted into position 32 of Switch I, in place of the normal tyrosine residue, showed little or no change in their tryptophan fluorescence, when comparing the GMP-PCP- and GDP-bound forms of the protein. These results again differed from those obtained with the corresponding Switch I mutant of H-Ras, which showed significant changes in the fluorescence of the Switch I tryptophan residue when comparing the GDP- and GMP-PCP-bound states.

Thus taken together, these findings raised the question as to how effector proteins are able to selectively recognize the GTP analog-bound form of Cdc42, and whether effectors might be capable of inducing and/or stabilizing specific conformational transitions within a Cdc42 species that appears to start off predominantly in a signaling-inactive conformation. Here we show that despite the GDP- and GMP-PCP-bound forms of Cdc42 sharing a similar Switch I conformational state, the tryptophan fluorescence of the GMP-PCP-bound Cdc42(Y32W) mutant undergoes a specific and significant change upon the binding of an effector protein. NMR experiments also showed that effector proteins were able to specifically promote conformational changes within Cdc42 molecules bound to GTP analogs. When this structure-function information is considered together with the structures for Cdc42 complexed to effectors that either use the conventional Cdc42/Rac-interactive binding (CRIB) domain, such as is the case for p21-activated kinase (Pak) (16), or a nonconventional Cdc42/Rac-binding domain, as occurs with Par6 (for Partitioning-defective protein-6) (17), it becomes apparent how effector proteins help to ensure that Cdc42 undergoes the necessary conformational changes for signal propagation.

Overall, our findings support the idea that there is a spectrum of possibilities regarding the conformational states that G-proteins can assume following the exchange of GDP for GTP (or GTP analogs), *i.e.* what is commonly referred to as the G-protein activation event. One end of the spectrum represents cases like Cdc42 where, in the absence of an effector protein, the majority of the population of the GTP-bound (or GTP analog-bound) G-protein exists in conformational states that are minimally changed from those for the GDP-bound form of the protein. Thus, Cdc42 relies heavily upon effector proteins to induce the correct conformational changes to enable signal propagation to occur. At the other end of the spectrum are the Gα subunits of heterotrimeric (large) G-proteins and small G-proteins like H-Ras where, upon GDP-GTP exchange, the majority of the G-protein population assumes conformational states that clearly differ from the GDP-bound protein and more closely approximate the signaling-active conformational states that are formed upon the binding of effectors.

EXPERIMENTAL PROCEDURES

Protein Purification—Escherichia coli cells expressing pET15b-his-Cdc42, pGEX-KG-Cdc42(Y32W,W97H), pGEX-KG-PBD(W98F), and pGEX-KG-PBD were grown at 37 °C until an OD of 0.8. Induction was initiated by the addition of isopropyl 1-thio-β-D-galactopyranoside (1 mM), and the cells were allowed to grow for another 3 h. Cells were pelleted at 6000 × *g* for 10 min and frozen at −80 °C. Cell pellets were homogenized in HMA buffer (20 mM Hepes, pH 8.0, 5 mM $MgCl_2$, 0.1 mM NaN_3) and lysed by sonication. Cell debris was centrifuged at 20,000 rpm for 30 min, and the supernatant was saved. Supernatants containing His_6-tagged Cdc42 were incubated briefly with chelating-Sepharose beads (Amersham Biosciences) charged with Ni^{2+} and equilibrated with HMA. Beads were washed with HMA plus 20 mM imidazole before elution with HMA plus 200 mM imidazole. GST-tagged proteins were incubated with glutathione beads (Amersham Biosciences) equilibrated with HMA for 30 min at 4 °C. Beads were washed with HMA containing 500 mM NaCl and again with HMA. Protein was eluted with 10 mM glutathione in HMA.

The His-tagged proteins were incubated with thrombin (Hematological Technologies Inc.) at 4 °C for 3–4 h. Clipped proteins were further purified by chromatography on a HiTrap Q column (Amersham Biosciences), and protein fractions were pooled.

Nucleotide Loading—Mutant and wild-type Cdc42 concentrations were measured using Bradford reagent (Pierce). Nonhydrolyzable nucleotide analogs were added to an ~5-fold excess relative to the protein concentration. Ammonium sulfate was added to a final concentration of 200 mM along with 100 units of alkaline phosphatase-bound acrylic beads (Sigma P0927). After a 4-h incubation at 4 °C, the beads were washed with HMA, and the flow-through was collected. The buffer was exchanged on a PD-10 column (Amersham Biosciences) equilibrated with HMA. Nucleotide content was confirmed by high pressure liquid chromatography analysis, using a previously published protocol (18).

GST-Cdc42 Pulldown Assays—Equal amounts of glutathione beads (Amersham Biosciences) were saturated with GST-Cdc42 bound to GMP-PCP, GMP-PNP, GTPγS, or GDP. After incubation for 1 h at 4 °C, the beads were washed three times with HMA, and an equivalent amount of the limit Cdc42/Rac-binding domain from Pak3 (PBD) was added to a 10-fold molar excess of Cdc42. Beads were washed three times with HMA after a 3-h incubation at 4 °C. Equal amounts of protein from each assay were boiled and loaded on a 4–20% gradient gel (Invitrogen).

X-ray Crystallography—Cdc42-GMP-PCP (80 mg/ml) crystals were grown in 12% PEG 6K, 100 mM ammonium sulfate, 100 mM sodium acetate, and 50 mM MES, pH 6.0, at 18 °C. Data were collected at the Cornell MacCHESS beamline A1 using an ADSC Quantumn-210 CCD Detector. Data processing was performed using Mosfilm, and initial phases were solved by molecular replacement using MolRep from the CCP4 suite (19). The model structure used to find the initial phases was Cdc42-GDP (PDB ID 1AN0) without nucleotide. Structure refinement was completed using CNS (20) and validated with Procheck (21).

^{31}P NMR—Samples were prepared by dissolving wild-type Cdc42 (1 mM) or the Cdc42(T35A) mutant pre-exchanged with GMP-PNP or GMP-PCP, either with or without the PBD (1 mM), in HMA containing 10% D_2O. ^{31}P spectra were obtained at 5 °C on a Varian INOVA spectrometer operating at 202.37 MHz using a 5-mm Varian DBG probe head. ^{1}H broadband decoupling was applied throughout the acquisition. A relaxation delay of 8 s was used between scans, with 3000–4000 scans summed prior to analysis. Data were zero-filled to 128K

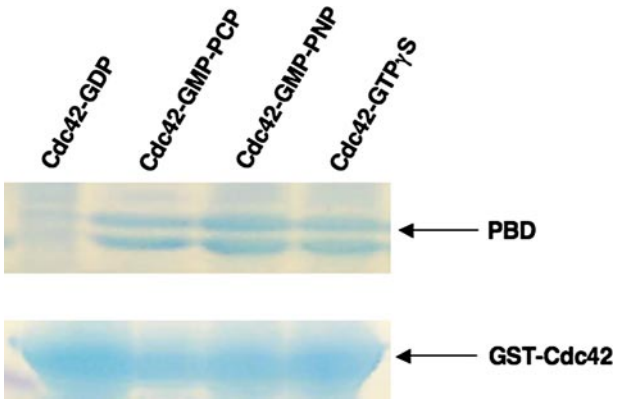

FIGURE 1. **Interactions between signaling-active forms of Cdc42 and the p21-binding domain of Pak3.** Glutathione beads were saturated with GST-Cdc42 (700 μg) bound to GDP, GMP-PCP, GMP-PNP, or GTPγS. Washed beads were incubated with a 10-fold molar excess of Pak3-PBD (p21-binding domain) for 3 h and washed. *1st lane* shows signaling-inactive Cdc42-GDP is ineffective at binding the effector protein. *2nd* to *4th lanes* show signaling-active Cdc42 is able to interact with PBD, which is detected as a doublet of 8–10 kDa.

points, and an exponential multiplication (5–10 Hz) was performed prior to Fourier transform. Spectra were referenced externally to 85% phosphoric acid (0 ppm).

Fluorescence Spectroscopy—All experiments were performed on a Varian Cary Eclipse fluorimeter. Excitation and emission slit widths were $\pm$5 and $\pm$10 nm, respectively. Cdc42 and H-Ras emission scan experiments were performed in HMA at 30 °C, using an excitation wavelength of 295 nm in HMA. Excitation and emission wavelengths for the binding assays of Cdc42(Y32W,W97H) with PBD(W98F) were 295 and 353 nm, respectively.

RESULTS

The X-ray Crystal Structure for GMP-PCP-bound Cdc42—The original x-ray crystal structures for the signaling-active (GTP-bound) form of H-Ras were obtained using the nonhydrolyzable GTP analogs GMP-PNP and GMP-PCP (11, 12), because GTP as well as GTPγS are hydrolyzed during the crystallization procedure. As is the case for Ras, these two nonhydrolyzable GTP analogs enable Cdc42 to interact with its downstream effector proteins. Fig. 1 presents some examples that show the selective ability of GST-Cdc42, when bound to different GTP analogs, to pull down the Cdc42/Rac-binding domains from Pak3 (*i.e.* the PBD), whereas the GDP-bound form of GST-Cdc42 was unable to bind to the effector. We therefore used the Cdc42-GMP-PCP complex for high resolution structural analysis of the signaling-active form of this G-protein.

Fig. 2*A* shows the ribbon diagram for the x-ray crystal structure for GMP-PCP-bound Cdc42 solved to 2.4 Å resolution (see Table 1 for statistics on data collection and refinement). The structure conforms to an α/β fold consisting of six β-strands, six α-helices, and one 3_{10} helix, and in general displays an architecture that is characteristic of other small G-proteins. Stabilization of the GMP-PCP molecule inside the nucleotide-binding pocket is achieved through hydrogen bonds between the guanine ring and surrounding residues, π-π stacking interactions with Phe-28, and hydrogen bonds with the phosphate oxygen atoms. Fig. 2*B* shows a representative electron density for a portion of the GMP-PCP-binding site.

There are two molecules of GMP-PCP-bound Cdc42 within the asymmetric unit. Crystal contacts involving Switch I from chain A help to stabilize the loop, specifically at residues Tyr-32 and Phe-37. A cleft is formed by Met-1, Pro-50, and Met-45 in a symmetry-related molecule which provides a hydrophobic interface for the phenyl group of Tyr-32 in Switch I. The formation of a hydrogen bond between Tyr-32 and Thr-35 from chain A helps to prevent Thr-35 from coordinating the Mg^{2+} (also see below), whereas Phe-37 is stabilized by π-π interactions with Tyr-64 from a symmetry-related molecule.

The individual temperature factors for residues within Switch I are higher than those found in adjacent areas of the protein where secondary structure stabilizes the residues. Moreover, the temperature factors for Switch I residues in chain B are higher than those for the corresponding residues in chain A. This is probably because of the fact that Phe-37 in chain B does not undergo π-π interactions with a symmetry-related molecule.

Comparisons of the Structures for the GMP-PCP- and GDP-bound Forms of Cdc42—Based on the x-ray crystallographic studies of H-Ras (11, 12) and various Gα subunits of the family of heterotrimeric or large G-proteins (13, 14), as well as the corresponding structures for the elongation factor Ef-Tu (10), it has been suggested that there are two conserved regions designated as Switch I and Switch II that undergo conformational changes as an outcome of GDP-GTP exchange (often referred to as the G-protein activation event). Thus, it has been generally assumed that changes occurring in Switch I and Switch II underlie the molecular switch function of both small and large G-proteins, enabling them to selectively engage their downstream signaling effector proteins. However, the x-ray crystal structure for the GMP-PCP-bound form of Cdc42 was immediately intriguing because when it was compared with signaling-inactive forms of Cdc42, these structural differences were not evident. The overall topology of the Cdc42-GMP-PCP complex, and its Switch I and II conformations in particular, were virtually identical to both the x-ray crystal structure that we had earlier solved for the GDP-bound form of Cdc42 (PDB ID 1AN0), as well as the reported structure for a signaling-inactive Cdc42(G12V)-GDP complex (22). Fig. 2*C* compares the Cdc42-GMP-PCP and Cdc42(G12V)-GDP complexes. A structural alignment of all the C-α atoms between these two complexes yielded an r.m.s.d. of ~0.75 Å.

The coordination of the Mg^{2+} ion is also virtually identical in the structures for the signaling-inactive GDP-bound form of Cdc42 *versus* the Cdc42-GMP-PCP complex (Fig. 2, *D* and *E*, respectively). It is interesting that in GMP-PCP-bound Cdc42, Thr-35 does not participate in Mg^{2+} coordination, given that it has been suggested to be critical for the structural change imparted by GTP analogs within the Switch I loop of H-Ras (23, 24). Specifically, Thr-35 appears to interact with the γ-phosphate of GTP in Ras with this interaction being lost upon GTP hydrolysis and thereby possibly accounting for the observed change in the orientation of Switch I. In the structure for the Cdc42-GMP-PCP complex, Thr-35 is not in position to coordinate the Mg^{2+} ion; however, a water molecule is visible and

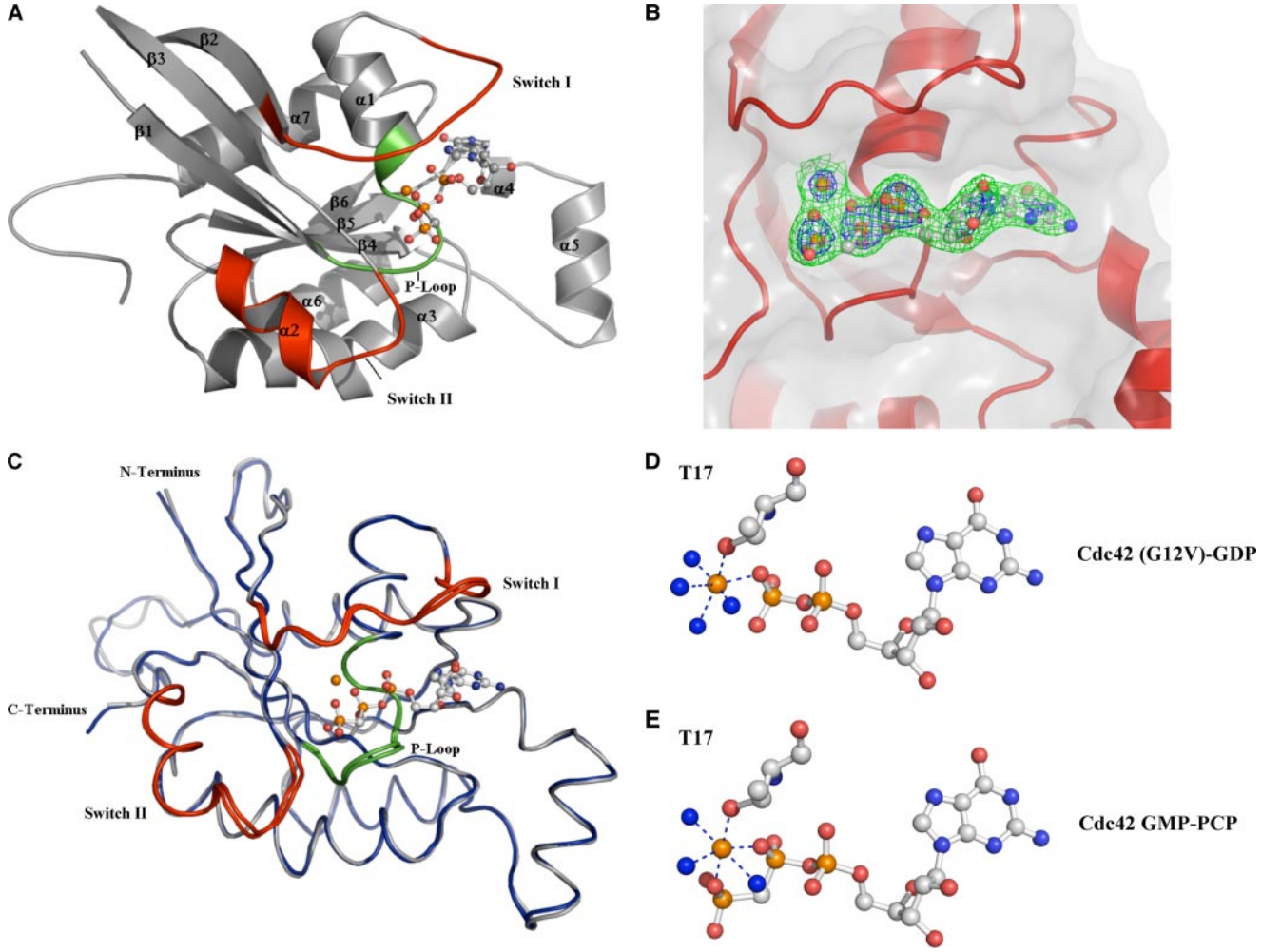

FIGURE 2. **X-ray crystal structure of GMP-PCP bound Cdc42 at 2.4 Å.** *A,* overall fold of GMP-PCP-bound Cdc42 is a classic G domain encompassing six β-sheets and five α-helices with a short two-helical insertion after the β-strand 5 known as the Rho insert region. The α-helix 4 is a short 3_{10} helix. Switch I and II are colored in *red* encompassing residues 30–37 and 60–70, respectively. P-loop residues, which are important for binding the phosphates, are colored *green*. *B,* electron density around the GMP-PCP is contoured at 1.5σ (*green*) and 4σ (*blue*) from a $2F_o - F_c$ map. Clear density is present for the γ-phosphate even at 4σ. *C,* structural alignment of the signaling-active Cdc42-GMP-PCP complex (*gray*) with the signaling-inactive Cdc42 (G12V)-GDP (*blue*). Switch regions and the P-loop are colored *red* and *green*, respectively. There is an overall r.m.s.d. of 0.75 Å for all C-α atoms between the two structures. *D* and *E,* close-up views of the Mg^{2+} coordination between the Cdc42 (G12V)-GDP and Cdc42-GMP-PCP structures, respectively. Phosphates and magnesium are shown in *orange*, and water and nitrogen molecules are colored *blue*. Threonine 35 does not coordinate to the γ-phosphate in the Cdc42-GMP-PCP structure as it does in other signaling active structures. It is replaced by a water molecule in the Cdc42 structures, whereas all other contacts are conserved. Figs. 2 and 3 were created with PyMOL (50).

TABLE 1
Data collection and refinement statistics for Cdc42-GMPPCP

Space group	$P4_12_12$
Unit cell (Å)	98.5, 98.5, 102.4
Resolution (Å)	2.4
Average redundancy (highest resolution)	4.1 (2.8)
$I/\sigma I$	6.8 (2)
R_{sym} [a] (highest resolution)(%)	6.8 (39)
Refinement Statistics	
Completeness %, (highest resolution)	95.5 (91.4)
Refinement resolution range (Å)	31–2.4
No. of reflections in working set	18,448 (95%)
No. of reflections in test set	991 (5%)
R_{free} [b] (%)	26
R_f [b] (%)	23
Ramachandran	
Most favored regions	87.3%
Allowed regions	12.3%
r.m.s.d. from ideal bond length (Å)	0.010
r.m.s.d. from ideal bond angle (°)	1.4

[a] $R_{sym} = \Sigma_{hkl}\Sigma_i[I_i(hkl) - \langle I(hkl)\rangle]/\Sigma_{hkl}\Sigma_i(hkl)$.
[b] R_{free} and $R_f = \Sigma|2F_o - F_c|/\Sigma F_o$.

substitutes for the hydroxyl group of the threonine residue. The same is true for the structure for the GDP-bound form of Cdc42, as well as for the Cdc42(G12V)-GDP complex (22).

The Cdc42-GMP-PCP complex crystallized in the same space group and unit cell dimensions as the Cdc42(G12V)-GDP complex. As a result, both the GDP- and GMP-PCP-bound Cdc42 structures share similar crystal contacts that help to stabilize Switch I. Many of these crystal contacts are absent in the second Cdc42-GMP-PCP molecule that is present within the asymmetric unit for the GTP analog-bound form of the G-protein. Although the electron density for Switch I from the second Cdc42 molecule shares a similar backbone conformation with Switch I from the first Cdc42 molecule within the asymmetric unit, it possesses elevated *B* factors. This leads us to suspect that Switch I is probably highly mobile in both the GDP- and GMP-PCP-bound forms of Cdc42, an idea supported by NMR findings (25, 26). Thus, crystal contacts have probably enabled us to

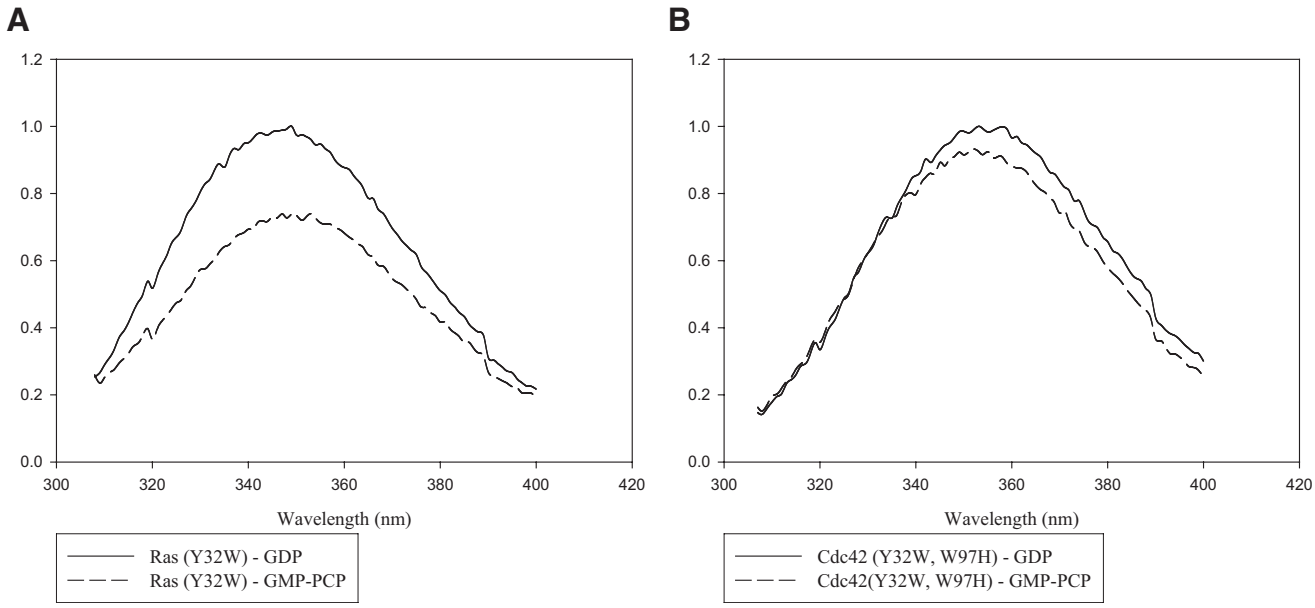

FIGURE 3. **Fluorescent spectra of the signaling-active and -inactive forms of Ras (Y32W) and Cdc42 (Y32W,W97H).** *A,* H-Ras(Y32W) (1 μM) bound to GDP (*top*) or GMP-PCP (*bottom*) was scanned at an excitation wavelength of 295 nm. A decrease in quantum yield of nearly 30% is observed upon binding of GMP-PCP. *B,* same experiments performed with the Cdc42(Y32W,W97H) mutant show that only a minor difference in quantum yield is observed between the GDP- and GMP-PCP-bound forms of the protein.

view one conformational state from possibly a number of states that may be shared by these two nucleotide-bound forms of Cdc42.

Fluorescence Studies of GDP-bound Versus GMP-PCP-bound Cdc42—We have taken advantage of the sensitivity of fluorescence spectroscopy to further examine the Switch I conformations for the GDP- and GMP-PCP-bound forms of Cdc42. The basic strategy was to first eliminate any background tryptophan fluorescence from Cdc42 by changing the tryptophan at position 97 to a histidine, and then to introduce a tryptophan residue at position 32 of Switch I, in place of the usual tyrosine residue. The expectation was that the Trp-32 residue would serve as a conformational probe for Switch I in Cdc42. This approach has been successfully used with H-Ras to detect conformational changes within Switch I upon GDP-GTP exchange (although in the case of H-Ras there are no tryptophan residues in the wild-type protein and so only the single substitution at position 32 was necessary) (27). Indeed, Fig. 3*A* shows that there is a significant difference in the intrinsic fluorescence measured for the H-Ras(Y32W) mutant when comparing its GDP- and GMP-PCP-bound states, such that the binding of the GTP analog results in an ~30% quenching in the Trp-32 fluorescence. On the other hand, the differences in the intrinsic fluorescence for the corresponding forms of the Cdc42(Y32W,W97H) mutant were much more subtle with GMP-PCP-bound Cdc42 showing at most a 5–10% decrease in Trp-97 fluorescence compared with its signaling-inactive, GDP-bound counterpart (Fig. 3*B*). Thus, these findings corroborated the results from x-ray crystal studies that showed the differences between the GDP- and GTP analog-bound forms of Ras were much more pronounced than the differences for the corresponding forms of Cdc42. Nonetheless, effector proteins are still able to distinguish between the GDP- and GMP-PCP-bound forms of Cdc42, as we observed a significant change in the fluorescence of the GMP-PCP-bound Cdc42(Y32W,W97H) protein (Fig. 4*A*), but not in the GDP-bound form of the protein (Fig. 4*B*), upon the addition of a recombinant form of the PBD in which its sole tryptophan residue was changed to a phenylalanine (PBD(W98F)). Successive additions of PBD(W98F) resulted in a dose-dependent quenching of the fluorescence from GMP-PCP-bound Cdc42(Y32W, W97H) that saturated at about 20% (Fig. 4*C*). Identical experiments were carried out with GMP-PNP-bound Cdc42(Y32W, W97H) with similar results (not shown). The NMR structure for GMP-PNP-bound Cdc42(Q61L) complexed to the CRIB domain of Pak1 shows that the nearest effector residue to position 32 in Switch I is ~12 Å away (16). The same is true when examining the coordinates from the recently determined x-ray structure for Cdc42-GMP-PCP bound to its limit-binding domain on Pak6 (PDB ID 2ODB). Thus, the fluorescence changes seen upon the addition of the PBD construct are likely a direct reflection of effector-induced conformational changes that are specific for the GTP analog-bound forms of Cdc42.

NMR Studies of Effector-induced Changes in GTP Analog-bound Forms of Cdc42—^{31}P NMR spectroscopy has proven to be very useful in studying the GTP-dependent activation of H-Ras in solution (23, 24). In particular, NMR studies led to the suggestion that the Ras-GMP-PNP complex exists in at least two conformational states (denoted as state 1 and state 2), as indicated by a split in the resonances of the β- and γ-phosphates of the GTP analog (23). More recently, a similar split in the phosphate resonances was detected when NMR analysis was applied to H-Ras bound to GMP-PCP (24). The addition of the limit Ras-binding domain from either of two Ras effectors, namely the Raf kinase or Ral-GDS, then pushed the equilibrium toward state 2. Therefore, state 2 for H-Ras is considered to represent the signaling-active species as seen in the x-ray crystal structures for the GTP analog-bound forms of the protein, whereas state 1 is thought to encompass an equilibrium of sub-

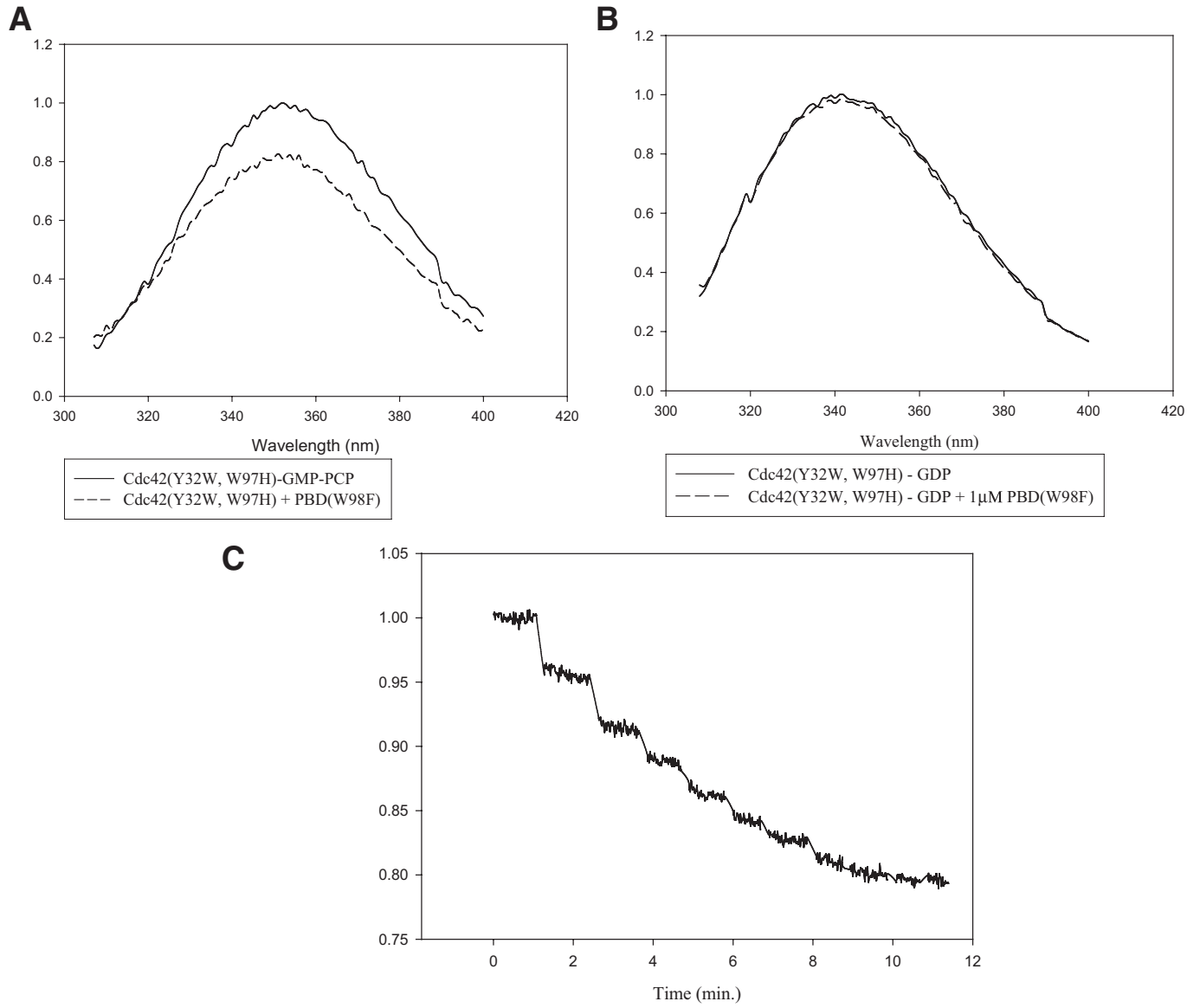

FIGURE 4. **Effector-induced changes in the Switch I conformation of GMP-PCP-bound Cdc42.** *A*, addition of the limit Cdc42/Rac-binding domain of Pak3 (PBD) (1 μM) to GMP-PCP-bound Cdc42(Y32W,W97H) (1 μM) causes a quenching of Trp-32 fluorescence. *B*, addition of the PBD to GDP-bound Cdc42(Y32W,W97H) has no effect on Trp-32 fluorescence. *C*, titration of GMP-PCP-bound Cdc42(Y32W,W97H) with increasing amounts of Pak3-PBD(W98F) (0.2–4 μM). The addition of PBD(W98F) decreases the quantum yield of the Cdc42 mutant until it reaches saturation at roughly 80% of the original intensity.

states that are in fast exchange on the NMR time scale and coincide with a marked decrease in affinity for all Ras effectors (28, 29).

Given these findings with H-Ras, we were interested in performing a similar analysis of Cdc42. As was done with H-Ras, we performed these experiments at 5 °C to slow down any interconversion that might occur between different conformational states of Cdc42, so that they could be detected on the NMR time scale. However, unlike the case for H-Ras, when we analyzed the complexes of Cdc42 bound to either GMP-PNP or GMP-PCP, we detected only a single peak for each phosphate (Fig. 5, *A* and *B*, respectively). These results indicated that the GTP analog-bound forms of Cdc42 assume only a single detectable conformational state in solution. Upon the addition of an equivalent molar amount of the PBD, conformational transitions were then detected in both the Cdc42-GMP-PNP (Fig. 5*A*) and Cdc42-GMP-PCP (Fig. 5*B*) complexes as indicated by shifts in the resonances for the γ-phosphate and to lesser extents for the β- and α-phosphates.

^{31}P NMR studies of the H-Ras Switch I mutant, H-Ras(T35A), suggested that this mutant resides exclusively in the signaling-defective state 1, even after the addition of an effector protein (24, 28, 29). It seemed likely that the same would be true for Cdc42, given that the yeast Cdc42(T35A) mutant was shown to be unable to sustain cell proliferation, polarization, or budding and to be defective in binding to all known yeast Cdc42 effectors (30), and so we examined the phosphate resonances for the human Cdc42(T35A) mutant in the presence and absence of the PBD. Fig. 5*C* shows that the resonances for the Cdc42(T35A)-GMP-PCP complex were slightly shifted when compared with those for GMP-PCP bound to wild-type Cdc42, suggesting that these two Cdc42

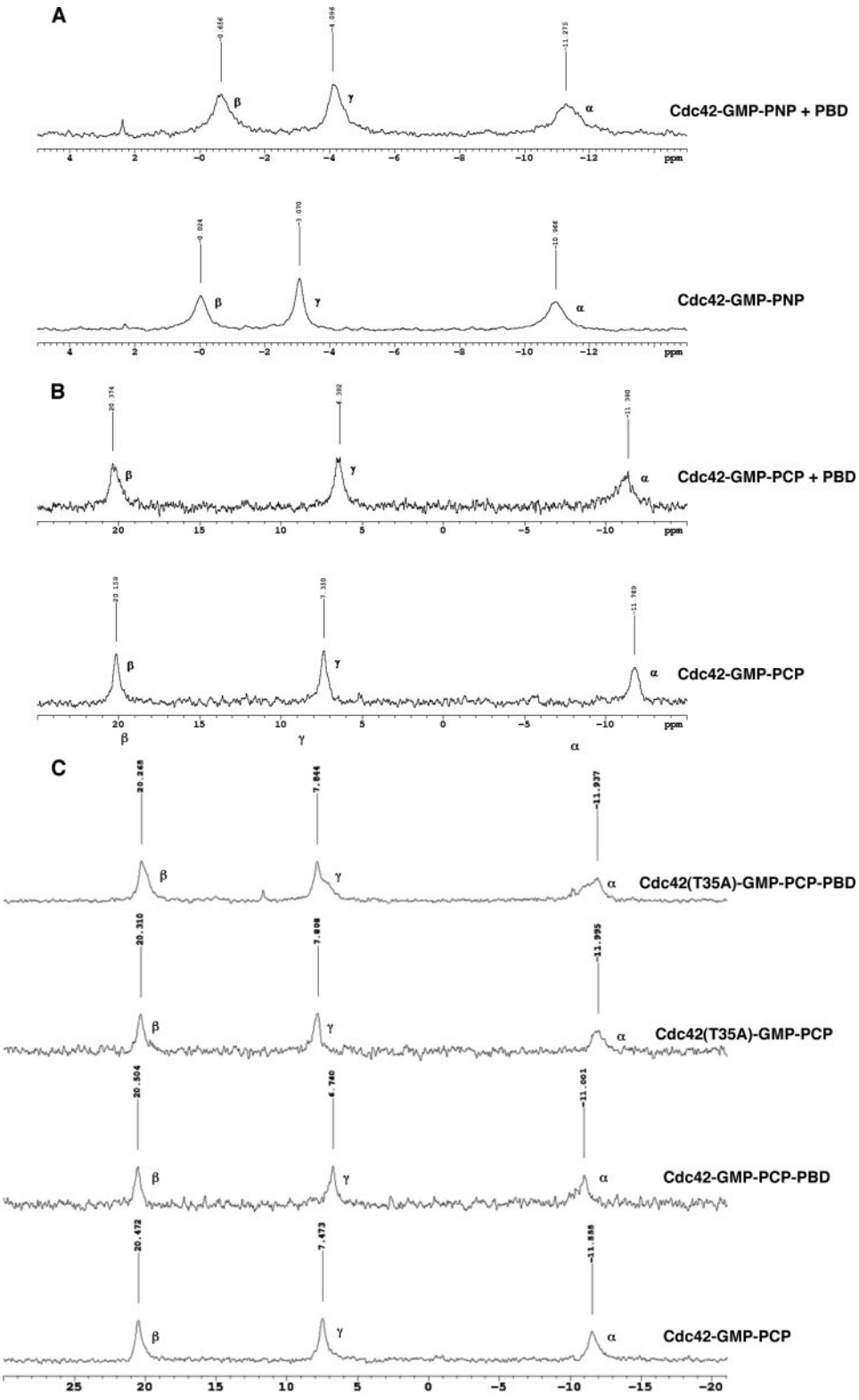

FIGURE 5. **^{31}P NMR reveals that Cdc42 exists only in one conformation in solution but assumes another upon addition of an effector.** *A*, Cdc42-GMP-PNP (0.75 mM) with (*top*) or without (*bottom*) Pak3-PBD (0.75 mM) at 5 °C. *B*, Cdc42-GMP-PCP (1 mM) with (*top*) or without (*bottom*) Pak3-PBD (1 mM) at 5 °C. A chemical shift of 1 ppm is seen for the γ-phosphate upon addition of the effector. Peaks are not split in any of the experiments implying Cdc42 has only one conformational state before binding the effector. *C*, comparison between Cdc42(T35A)-GMP-PCP (1 mM) (*top*) and Cdc42-GMP-PCP (1 mM) (*bottom*) with or without Pak3-PBD (1 mM).

species may start off in very similar, albeit subtly different, conformational states (Fig. 5*C*). However, importantly, the addition of the PBD did not cause a clearly detectable change in the positions of the peaks for the phosphate resonances for the GMP-PCP-bound Cdc42(T35A) mutant but only an overall broadening of the lines, whereas in the same experiment, the addition of the PBD caused obvious changes in the peak positions for the phosphate resonances for the GMP-PCP-bound wild-type Cdc42. These findings suggest that the GMP-PCP-bound Cdc42(T35A) mutant has a weaker affinity for the PBD because of the loss of stabilizing interactions from Thr-35 to the Mg^{2+}.

Insights into the Mechanism by Which Activated Cdc42 Propagates Signals to Its Downstream Effector Proteins—Based on the results from our fluorescence and NMR studies, it would appear that effector proteins play a major role in selectively inducing and/or stabilizing the signaling-active conformational states of Cdc42. Various lines of evidence also indicate that both the signaling-inactive (GDP-bound) and signaling-active (GMP-PCP-bound) forms of Cdc42 have Switch regions that are highly mobile and likely encompass very similar, or at least overlapping, conformational equilibria (25, 26). This then raises a key question: how are effectors able to distinguish between the GDP- and GTP analog-bound forms of Cdc42, such that they interact with the latter Cdc42 species with high affinity? Given the plasticity of Switch I, it is possible that key residues such as Val-36 or Phe-37 may be oriented in such a way as to be recognizable to effectors, when Cdc42 is bound to either GDP or GTP analogs. However, presumably the effector would then only be able to engage the GTP analog-bound form of Cdc42 in a manner that results in a high affinity, signaling-competent interaction. Careful comparisons of the structure for Cdc42-GMP-PCP with those for different Cdc42-ef-

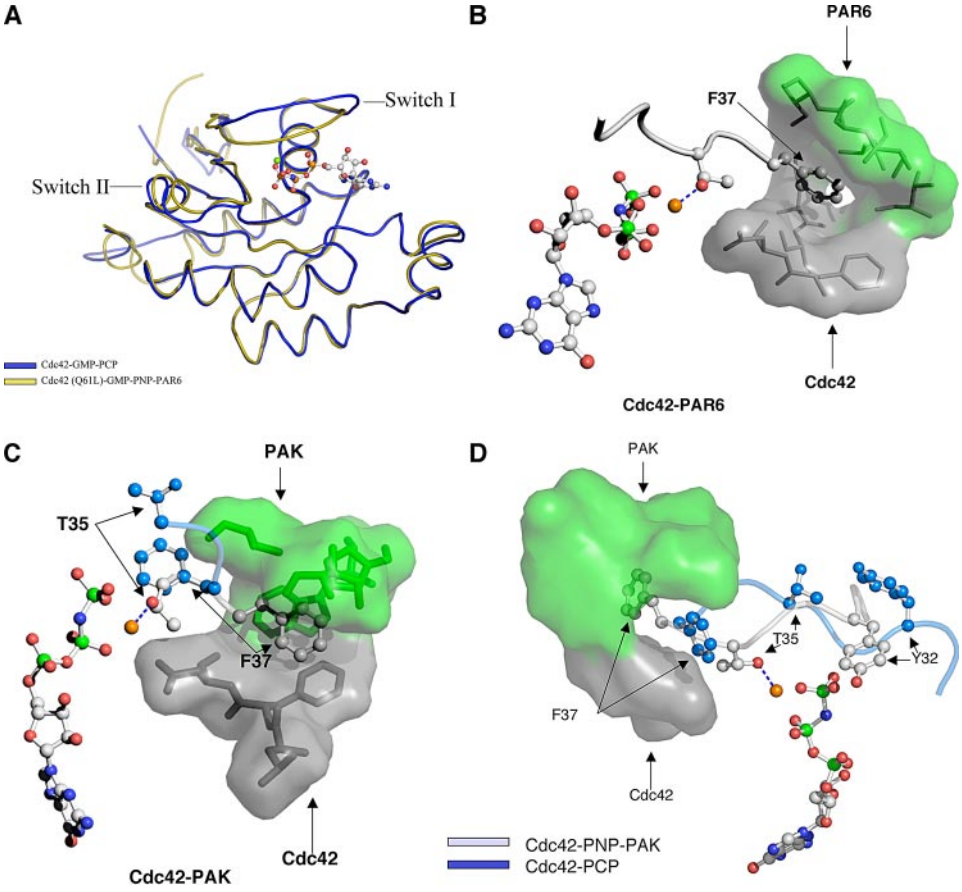

FIGURE 6. **Effector proteins stabilize Switch I in an "active" conformation.** *A*, comparisons of the overall fold of GMP-PCP-bound Cdc42 *versus* GMP-PNP-bound Cdc42(Q61L) complexed to Par6 (PDB ID 1NF3). *B*, Switch I residues Thr-35 and Phe-37 for Cdc42(Q61L)-GMP-PNP bound to the nonconventional Cdc42/Rac-interactive-binding domain of Par6 are shown in *gray*. Par6 residues (in *green*) form the lid to a hydrophobic pocket for Phe-37, with the bottom of the pocket being contributed by residues from Cdc42 (*gray*). Phe-37 acts as a fulcrum lever to flip Thr-35 into position to coordinate the Mg^{2+}. *C*, same view of Cdc42(Q61L)-GMP-PNP bound to the CRIB domain of Pak1 based on the NMR structure for this complex (PDB ID 1E0A). Phe-37 is embedded in a hydrophobic pocket created by both Pak1 (*green*) and Cdc42 (*gray*). An overlay of Thr-35 and Phe-37 from Cdc42-GMP-PCP is displayed in *blue* to illustrate the lever action and stabilization of Phe-37 by Pak. *D*, overlay of Switch I from the NMR structure for the Cdc42-GMP-PNP-Pak1 complex (PDB ID 1E0A) and the x-ray structure for the Cdc42-GMP-PCP complex. Notice that in the Pak1 complex, Switch I residues from Cdc42 are rotated 180° from their position in the Cdc42-GMP-PCP structure and are stabilized by the interaction of Phe-37 with the effector protein.

fector complexes (16, 17, 31, 32) suggest how this might occur. An example is shown in Fig. 6*A*, which compares the overall topology for the Cdc42-GMP-PCP complex with that determined from the x-ray structure for the complex between GMP-PNP-bound Cdc42(Q61L) and the effector protein Par6. Although the two structures show little differences in Switch II, they highlight an obvious change in the Switch I effector loop. These differences, when considered together with the available x-ray and NMR structures for other complexes between Cdc42 and effector proteins, suggest the following sequence of events for how effectors are able to selectively bind with high affinity to the GTP-bound state of Cdc42. The first step involves the formation of a small hydrophobic pocket that buries either Switch I residue Phe-37 or Val-36, or both. Fig. 6*B* depicts this step for Par6, whereas Fig. 6*C* shows another example for one of the better known effectors for Cdc42, Pak1 (p21-activated kinase-1). In both of these cases, residues from the effector proteins (Fig. 6, *B* and *C*, shown in *green*) contribute to the lid of the binding-pocket, whereas residues from Switch II of Cdc42 (shown in *gray*) form the bottom of the pocket. The potential role for the hydrophobic pocket is to stabilize Switch I residues, and in particular to enable Phe-37 to act as a lever to flip Switch I, effectively reversing the orientations of key residues when compared with the signaling-inactive (GDP-bound) forms of the protein. This rearrangement, which is depicted in Fig. 6*D* for the case of Cdc42 binding to Pak1, allows Tyr-32 as well as Thr-35 to coordinate the γ-phosphate and Mg^{2+} ion, respectively, and to lock the signaling-active conformation in place. When the nucleotide in the binding pocket is GDP (instead of GTP), the absence of the γ-phosphate would not allow these stabilizing interactions with Switch I residues, and as a result, the effector is not able to bind with high affinity. Likewise, the Cdc42(T35A) mutant, which lacks the critical Switch I threonine residue, is defective in its ability to assume a stable activated conformational state in the presence of effector proteins (Fig. 5*C*).

It should be noted that this pattern of recognition of the GTP-bound state of Cdc42 is also used by the Cdc42-GAP (33). In this case, residues from the GAP together with Switch II form a pocket that buries Phe-37, with a network of interactions involving Arg-305 from the GAP (*i.e.* the "arginine finger") linking Switch I and Switch II residues with the γ-phosphate.

DISCUSSION

Structural studies performed on H-Ras and various members of the large heterotrimeric G-protein family demonstrated that there were two conserved regions (Switch I and Switch II) that changed conformation upon GDP-GTP exchange (11–14). These conformational "hot spots" have been assumed to represent the basis by which G-proteins act as molecular switches in cellular signaling pathways, by binding and regulating the activities of their biological effectors. GMP-PCP-bound Cdc42 is able to recognize effector proteins similar to other signaling-active forms of Cdc42 that contain bound GTP or other GTP analogs, and in a manner distinct from the signaling-inactive GDP-bound Cdc42. Thus, it was surprising when we determined a high resolution x-ray crystal structure for Cdc42 bound to the GTP analog GMP-PCP and found that it was virtually identical, including its Switch I and Switch II regions,

to the corresponding structures for signaling-inactive, GDP-bound forms of the protein (*i.e.* both wild-type Cdc42-GDP and Cdc42(G12V)-GDP).

Studies performed in solution further supported the conclusions that we reached from an analysis of the x-ray structures. We introduced a tryptophan residue at position 32 within Switch I, to use its intrinsic fluorescence properties as a conformational monitor for changes that occur within this region of Cdc42 following GDP-GTP exchange, as well as upon the ensuing binding of an effector protein. In these studies, we saw little if any change in the Switch I conformation of Cdc42 when comparing the GDP- and GMP-PCP-bound states of the protein (*i.e.* on the order of at most 5–10%). Here again this differed from the case for H-Ras, as we and others have been able to detect more significant differences in the Switch I conformation (*i.e.* ≥30%) when using a similar fluorescence readout to compare the GDP- and GTP analog-bound states of the protein. We then showed by using ^{31}P NMR spectroscopy that unlike the case for H-Ras, where two distinct states were detected for GTP analog-bound forms of the G-protein (24, 28, 34), with one of these apparently representing the signaling-active state, both the GMP-PNP- and GMP-PCP-bound forms of Cdc42 exhibited only a single (nonactivated) conformational state.

Despite the structural similarities between the GDP- and GMP-PCP-bound forms of Cdc42, effector proteins are able to distinguish between these two species. When the limit-binding domain of Pak3 was added to the GMP-PCP-bound form of the Cdc42(Y32W,W97H) protein, a clear change in the fluorescence emission from the Switch I tryptophan residue was observed, whereas the effector protein had no effect on the fluorescence emission of the GDP-bound Cdc42(Y32W, W97H) mutant. The addition of the effector protein also caused shifts in the phosphate resonances for the GMP-PCP- and GMP-PNP-bound forms of Cdc42 as readout by NMR spectroscopy. The latter findings are consistent with various other lines of evidence from NMR studies. The NMR-derived structures for different activated forms of Cdc42 bound to WASP (Wiscott-Aldrich syndrome protein), Pak, and Ack (activated Cdc42-associated kinase) showed no resonances for either the Switch I or Switch II regions of Cdc42, prior to the addition of the effector protein (16, 31, 32, 35). This was attributed to the dynamic nature of these regions. However, upon the addition of a Cdc42-effector protein, the resonances for these regions then became clearly defined (16, 31, 32, 35). Additionally, Oswald and co-workers (26) demonstrated in NMR studies that Switch I and Switch II contained significant flexibility and exhibited rapid conformational exchange in both the GDP- and GMP-PCP-bound forms of Cdc42, and that this flexibility was reduced in the Cdc42-GMP-PCP species upon the binding of an effector.

Taken together, these findings highlight the strong influence exerted by effector proteins on Cdc42 and its ability to assume signaling-active conformational states. However, the role of effector proteins in influencing such conformational transitions is not restricted to Cdc42, as fluorescence and NMR studies have shown that effectors also affect the signaling-active states of H-Ras (24, 28, 29, 36–38). As alluded to above, the results from NMR experiments showed that upon binding GTP analogs, H-Ras can exist in two stable conformational states. The majority of the GTP analog-bound H-Ras population appeared to assume what was felt to be a signaling-active conformational state (state 2), with the remainder of the H-Ras molecules being in a signaling-inactive conformation (state 1). The binding of the limit-functional domain from a Ras effector (*e.g.* the Raf serine/threonine kinase) then promoted and/or stabilized the signaling-active state 2 conformation, such that the total H-Ras population assumed this state in the presence of the effector (24). Interestingly, the NMR results reported for M-Ras were similar to what we have seen for Cdc42; specifically, GMP-PNP-bound M-Ras showed only a single stable conformational state as detected by ^{31}P NMR, which was then altered upon the addition of the effector protein Raf (36). Still, the x-ray crystal structures for the GDP- and GMP-PNP-bound forms of M-Ras showed changes in Switch I. The authors concluded that upon binding GTP analogs essentially the entire pool of M-Ras adopts the signaling-inactive state 1 conformation originally described for H-Ras, and that the binding of effector proteins then drives the GTP analog-bound forms of M-Ras entirely to the signaling-active state 2 conformation. What distinguishes the findings that we report here for Cdc42 is that both the state 1 and state 2 conformations for the GTP analog-bound Ras proteins can be structurally distinguished from GDP-bound Ras, although we are able to detect little if any structural differences between the GDP- and GMP-PCP-bound forms of Cdc42. Nonetheless, effector proteins are able to distinguish between these two forms of Cdc42.

An important question concerns whether the apparent strong reliance exhibited by Cdc42 for effector-induced conformational changes occurs in cells with the physiologically relevant, activating nucleotide GTP. In fact, it has been reported that the equilibrium constants for the inter-conversion between the inactive and active states of H-Ras, as measured by ^{31}P NMR (*i.e.* states 1 and 2, respectively), are higher for H-Ras bound to GMP-PCP or GMP-PNP when compared with GTP (24). We have tried to use fluorescence spectroscopy to see whether Cdc42 might behave differently when bound to GTP, compared with the nonhydrolyzable analogs GMP-PCP or GMP-PNP. Thus far, these experiments have been inconclusive. Similar to what we have seen with the nonhydrolyzable GTP analogs, we have been unable to detect a significant difference in the fluorescence emission from Trp-32 between the GDP-bound and GTP-bound Cdc42(Y32W,W97H) species. However, as yet we have not been able to observe reliable differences in the Trp-32 fluorescence upon the addition of the limit-binding domain of Pak3. At least part of the challenge in making interpretations from these experiments comes from the fact that Cdc42 shows a significantly higher intrinsic GTP hydrolytic activity compared with H-Ras (39), which may obscure differences, such as those induced by effector proteins. Still, the fact that effectors have a clear and substantial influence on the final conformational state that Cdc42 is able to assume in the presence of nonhydrolyzable GTP analogs that are signaling-competent leads us to believe that effector proteins will play a similarly important role for GTP-bound Cdc42 in the cell.

All of this leads to yet another interesting question, namely how do effector proteins select between the GDP- and GTP-bound forms of Cdc42, so as to ensure that signals are only transmitted when this G-protein is in the GTP-bound state? We obtained some clues toward answering this question when considering the available structures for GTP analog-bound forms of Cdc42 in complexes with the limit domains of different effector proteins. For each of these cases, the effector provides a binding pocket for Phe-37 of Switch I of Cdc42, which then leads to an interaction between Thr-35 from Switch I and the γ-phosphate of the GTP analog. In solution, the Switch I loop of Cdc42 is highly mobile and is likely able to interconvert between different conformations representing local minima on the energy landscape. Some of these minima may represent signaling conformations that can be reached by both the GDP- and GMP-PCP-bound proteins and enable the proper presentation of Phe-37 to be "captured" by the effector protein. Once this occurs, it creates a domino effect whereby important residues such as Thr-35 as well as Tyr-32 are brought into close contact with the nucleotide. The net outcome is that Cdc42 is locked into a complex with the effector, but only when it contains the γ-phosphate of GTP.

The role played by Phe-37 in forming a high affinity complex with effectors probably explains our earlier observations that this residue is essential for Cdc42-coupled signaling events linked to cell growth and cellular transformation (40). Also in support of this model, we showed in NMR studies that the GMP-PCP-bound Cdc42(T35A) mutant was not able to respond to effectors in the same way as the wild-type Cdc42-GMP-PCP complex. Specifically, the addition of the PBD to GMP-PCP-bound Cdc42(T35A) did not cause distinct shifts in the phosphate resonances, unlike the case for the wild-type Cdc42-GMP-PCP species, but did cause some line broadening. This suggests that the effector is able to interact with the Cdc42(T35A)-GMP-PCP complex but with a much weaker affinity compared with GMP-PCP-bound wild-type Cdc42. Therefore, in the absence of the critical Switch I Thr-35 residue, the GMP-PCP-bound Cdc42 mutant was unable to be locked into a high affinity, signaling-active conformational state by the effector. The fact that we observed slightly different peak positions for the phosphate resonances from the Cdc42(T35A)-GMP-PCP complex *versus* the Cdc42-GMP-PCP complex would suggest that these two Cdc42 species do not share identical conformational profiles, even though they both exist primarily in signaling-inactive states. What nonetheless seems clear from comparisons of the x-ray structures for the GDP- and GMP-PCP-bound forms of Cdc42, as well as from fluorescence and NMR studies, is that the spectrum of conformational states for these different nucleotide states of Cdc42 must overlap and that the Switch conformations for the wild-type Cdc42-GMP-PCP complex and the GDP-bound Cdc42 species are more closely related than those for GMP-PCP-bound Cdc42 before and after the binding of effectors.

The results that we have obtained regarding the conformational status of the Switch regions of Cdc42 in response to GDP-GTP exchange, *versus* the changes induced by biological effectors, are consistent with the biochemical and structural analyses of the interactions of Cdc42 with RhoGDI. Both the GDP- and GTP-bound states of Cdc42 are regulated by RhoGDI, such that the GDI significantly slows their rates of GDP dissociation and GTP hydrolysis (41, 42). Fluorescence measurements have shown that RhoGDI binds to the GDP- and GTP-bound forms of Cdc42 with identical affinities, at least in solution (43). This might be explained by the fact that Switch II looks identical when comparing the x-ray crystal structure for the Cdc42-GDP-RhoGDI complex (44) with that for GMP-PCP-bound Cdc42. Switch II represents the initial site of contact for RhoGDI and so the lack of any detectable change in this region when comparing GDP- and GTP-bound forms of Cdc42 would be consistent with the inability of the GDI to distinguish between these different states of the G-protein. What is especially interesting is that Switch II also shows little or no change when comparing the GDP- and GTP-bound forms of Cdc42 with any of the reported x-ray crystal structures for Cdc42 complexed to effector proteins.

Given these findings, it becomes interesting to consider whether G-proteins related to Cdc42 might show a similar behavior with regard to their Switch domains, and thus rely heavily on effector proteins to induce the necessary changes to ensure signal propagation. One such related G-protein is Rac1, which is 68% identical to Cdc42 and shares some of the same effector proteins. In the case of the x-ray crystal structure for GMP-PNP-bound Rac1, Switch I residues Tyr-32 through Val-36 exhibited poor electron density and consequently this region was modeled in the completed structure by using data from the related *Dictyostelium discoideum* protein Rac1a (45). This makes it difficult to know with certainty whether Switch I changes in the x-ray crystal structures for the GTP analog- and GDP-bound forms of Rac1. However, it is interesting that the x-ray structures for the GDP- and GMP-PNP-bound forms of Rac1, when complexed to the putative Rac-effector Arfaptin, are nearly identical (46). Moreover, Thr-35 from Switch I does not participate in coordinating the Mg^{2+} ion in either the GDP- or GMP-PNP-bound Rac1-Arfaptin structures, which is in contrast to what is typically seen in the structures of all small G-proteins when they are in their signaling-active states. These results would seem to suggest that GDP-GTP exchange on Rac1 is not sufficient to induce significant conformational changes within the Switch I region of the protein.

The x-ray crystal structures for the GDP and GTP analog-bound forms of RhoA show that changes in the Switch I loop do occur within this G-protein as an outcome of GDP-GTP exchange (47). On the other hand, our recent studies with RhoC suggest that it can exist in multiple activated states and that effector proteins again influence the final conformational states that are reached and necessary for signal propagation (48).

Thus, it is becoming increasingly clear that a spectrum of possibilities exist regarding how G-proteins reach the conformational states that are necessary for signal propagation. At one end of the spectrum are the α subunits of large G-proteins (Gα subunits), for which the conformational changes necessary for signal propagation may be entirely driven by GDP-GTP exchange. Indeed, the ability of Gα subunits to undergo such conformational transitions is necessary for

their signaling function, as the GDP-bound Gα subunits are tightly associated with their partner G$\beta\gamma$ complexes and movements in Switch II that accompany GDP-GTP exchange are thought to be necessary to reduce the affinity of G$\beta\gamma$ and enable the GTP-bound Gα subunit to engage its downstream signaling effector. For the case of H-Ras, GDP-GTP exchange may be sufficient to induce differences in Switch I and Switch II within a significant population of the G-protein molecules that can be recognized by many of their effector proteins. A number of these effectors (*e.g.* Raf, phosphatidylinositol 3-kinase, and Ral-GDS) appear to use a similar mode of binding, so each might even be able to recognize the same GTP-induced conformational state within the G-protein (49). Still, the principal site for effector binding in Ras (Switch I) is a highly flexible region, given that two conformational states have been detected for GTP analog-bound forms of H-Ras from NMR studies, such that the binding of effectors can induce and/or stabilize one of these states and thereby ensure that the vast majority of GTP analog-bound H-Ras molecules are in a signaling-active conformation (24).

Cdc42 may represent an example of a G-protein that is at the other end of the spectrum, as its GTP-bound state appears to be strongly receptive to effector-induced conformational changes. It may be especially important that the effector-binding site on Cdc42 shows significant plasticity, given that the GTP-bound form of this protein engages a number of different cellular effectors. Moreover, Cdc42 needs to move between distinct cellular compartments to activate specific effector proteins (*e.g.* between the plasma membrane and Golgi), and this movement may be mediated by RhoGDI, which, as alluded to above, binds to both the signaling-inactive and signaling-active forms of the G-protein (3). Thus, the ability of individual effector proteins to mold Cdc42 into a favorable conformational state for different signaling events would be highly advantageous by providing maximum flexibility for a G-protein that needs to switch on a number of effector activities located at different sites within the cell.

Acknowledgments—We thank Tony Condo at the Cornell NMR Facility for expertise and help with all of the ^{31}P NMR experiments. We also thank Cindy Westmiller and Debbie Crane for their expert secretarial assistance.

REFERENCES

1. Johnson, D. I. (1999) *Microbiol. Mol. Biol. Rev.* **63,** 54–105
2. Nobes, C. D., and Hall, A. (1995) *Biochem. Soc. Trans.* **23,** 456–459
3. Cerione, R. A. (2004) *Trends Cell Biol.* **14,** 127–132
4. Barbacid, M. (1987) *Annu. Rev. Biochem.* **56,** 779–827
5. Cerione, R. A., and Zheng, Y. (1996) *Curr. Opin. Cell Biol.* **8,** 216–222
6. Whitehead, I. P., Campbell, S., Rossman, K. L., and Der, C. J. (1997) *Biochim. Biophys. Acta* **1332,** 1–23
7. Erickson, J. W., and Cerione, R. A. (2004) *Biochemistry* **43,** 837–842
8. Erickson, J. W., and Cerione, R. A. (2001) *Curr. Opin. Cell Biol.* **13,** 153–157
9. Scheffzek, K., Ahmadian, M. R., and Wittinghofer, A. (1998) *Trends Biochem. Sci.* **23,** 257–262
10. Jurnak, F. (1985) *Science* **230,** 32–36
11. de Vos, A. M., Tong, L., Milburn, M. V., Matias, P. M., Jancarik, J., Noguchi, S., Nishimura, S., Miura, K., Ohtsuka, E., and Kim, S. H. (1988) *Science* **239,** 888–893
12. Pai, E. F., Kabsch, W., Krengel, U., Holmes, K. C., John, J., and Wittinghofer, A. (1989) *Nature* **341,** 209–214
13. Noel, J. P., Hamm, H. E., and Sigler, P. E. (1993) *Nature* **366,** 654–663
14. Coleman, D. E., Berghuis, A. M., Lee, E., Linder, M. E., Gilman, A. G., and Sprang, S. R. (1994) *Science* **265,** 1405–1412
15. Milburn, M. V., Tong, L., deVos, A. M., Brunger, A., Yamaizumi, Z., Nishimura, S., and Kim, S. H. (1990) *Science* **247,** 939–945
16. Morreale, A., Venkatesan, M., Mott, H. R., Owen, D., Nietlispach, D., Lowe, P. N., and Laue, E. D. (2000) *Nat. Struct. Biol.* **7,** 384–388
17. Garrard, S. M., Capaldo, C. T., Gao, L., Rosen, M. K., Macara, I. G., and Tomchick, D. R. (2003) *EMBO J.* **22,** 1125–1133
18. Majumdar, S., Ramachandran, S., and Cerione, R. A. (2006) *J. Biol. Chem.* **281,** 9219–9226
19. Collaborative Computational Project, Number 4 (1994) *Acta Crystallogr. Sect. D Biol. Crystallogr.* **50,** 760–763
20. Brunger, A. T., Adams, P. D., Clore, G. M., DeLano, W. L., Gros, P., Grosse-Kunstleve, R. W., Jiang, J. S., Kuszewski, J., Nilges, M., Pannu, N. S., Read, R. J., Rice, L. M., Simonson, T., and Warren, G. L. (1998) *Acta Crystallogr. Sect. D Biol. Crystallogr.* **54,** 905–921
21. Morris, A. L., MacArthur, M. W., Hutchinson, E. G., and Thornton, J. M. (1992) *Proteins* **12,** 345–364
22. Rudolph, M. G., Wittinghofer, A., and Vetter, I. R. (1999) *Protein Sci.* **8,** 778–787
23. Geyer, M., Schweins, T., Herrmann, C., Prisner, T., Wittinghofer, A., and Kalbitzer, H. R. (1996) *Biochemistry* **35,** 10308–10320
24. Spoerner, M., Nuehs, A., Ganser, P., Herrmann, C., Wittinghofer, A., and Kalbitzer, H. R. (2005) *Biochemistry* **44,** 2225–2236
25. Feltham, J. L., Dötsch, V., Raza, S., Manor, D., Cerione, R. A., Sutcliffe, M. J., Wagner, G., and Oswald, R. E. (1997) *Biochemistry* **36,** 8755–8766
26. Loh, A. P., Guo, W., Nicholson, L. K., and Oswald, R. E. (1999) *Biochemistry* **38,** 12547–12557
27. Resland, H., John, J., Linke, R., Simon, I., Schlichting, I., Wittinghofer, A., and Goody, R. S. (1995) *Biochemistry* **34,** 593–599
28. Spoerner, M., Wittinghofer, A., and Kalbitzer, H. R. (2004) *FEBS Lett.* **578,** 305–310
29. Spoerner, M., Herrmann, C., Vetter, I. R., Kalbitzer, H. R., and Wittinghofer, A. (2001) *Proc. Natl. Acad. Sci. U. S. A.* **98,** 4944–4949
30. Gladfelter, A. S., Moskow, J. J., Zyla, T. R., and Lew, D. J. (2001) *Mol. Biol. Cell* **12,** 1239–1255
31. Abdul-Manan, N., Aghazadeh, B., Liu, G. A., Majumdar, A., Ouerfelli, O., Siminovitch, K. A., and Rosen, M. K. (1999) *Nature* **399,** 379–383
32. Mott, H. R., Owen, D., Nietlispach, D., Lowe, P. N., Manser, E., Lim, L., and Laue, E. D. (1999) *Nature* **399,** 384–388
33. Nassar, N., Hoffman, G., Manor, D., Clardy, J. C., and Cerione, R. A. (1998) *Nat. Struct. Biol.* **5,** 1047–1052
34. Stumber, M., Geyer, M., Graf, R., Kalbitzer, H. R., Scheffzek, K., and Haeberlen, U. (2002) *J. Mol. Biol.* **323,** 899–907
35. Gizachew, D., Guo, W., Chohan, K. K., Sutclifee, M. J., and Oswald, R. E. (2000) *Biochemistry* **39,** 3963–3971
36. Ye, M., Shima, F., Muraoka, S., Liao, J., Okamoto, H., Yamamoto, M., Tamura, A., Yagi, N., Ueki, T., and Kataoka, T. (2005) *J. Biol. Chem.* **280,** 31267–31275
37. Herrmann, C., Horn, G., Spaargaren, M., and Wittinghofer, A. (1996) *J. Biol. Chem.* **271,** 6794–6800
38. Sydor, T., Engelhard, M., Wittinghofer, A., Goody, R. S., and Herrmann, C. (1998) *Biochemistry* **37,** 14292–14299
39. Hart, M. J., Shinjo, K., Hall, A., Evans, T., and Cerione, R. A. (1991) *J. Biol. Chem.* **266,** 20840–20848
40. Wilson, K. W., Wu, W. J., and Cerione, R. A. (2000) *J. Biol. Chem.* **275,** 37307–37310
41. Hart, M. J., Maru, Y., Leonard, D., Witte, O. N., Evans, T., and Cerione, R. A. (1992) *Science* **258,** 812–815
42. Leonard, D. A., Hart, M. J., Platko, J. V., Eva, A., Henzel, W., Evans, T., and Cerione, R. A. (1992) *J. Biol. Chem.* **267,** 22860–22868
43. Nomanbhoy, T. K., and Cerione, R. (1996) *J. Biol. Chem.* **271,** 10004–10009

44. Hoffman, G. R., Nassar, N., and Cerione, R. A. (2000) *Cell* **100,** 345–356
45. Hirshberg, M., Stockley, R. W., Dodson, G., and Webb, M. R. (1997) *Nat. Struct. Biol.* **4,** 147–152
46. Tarricone, C., Xiao, B., Justin, N., Walker, P. A., Rittinger, K., Gamblin, S. J., and Smerdon, S. J. (2001) *Nature* **411,** 215–219
47. Ihara, K., Muraguchi, S., Kato, M., Shimizu, T., Shirakawa, M., Kuroda, S., Kaibuchi, K., and Hakoshima, T. (1998) *J. Biol. Chem.* **273,** 9656–9666
48. Dias, S. M., and Cerione, R. A. (2007) *Biochemistry* **46,** 6547–6558
49. Wittinghofer, A., and Nassar, N. (1996) *Trends Biochem. Sci.* **21,** 488–491
50. DeLano, W. L. (2002) *The PyMOL Molecular Graphics System*, San Carlos, CA